JOURNAL OF CATALYSIS 95, 414–422 (1985)

A Spectroscopic Study of the Effect of H_2O and NiO on the Surface Structure of $NiO–MoO_3/Al_2O_3$[1]

J. M. STENCEL, L. E. MAKOVSKY, J. R. DIEHL, AND T. A. SARKUS

Pittsburgh Energy Technology Center, P.O. Box 10940, Pittsburgh, Pennsylvania 15236

Received March 8, 1985; revised May 1, 1985

The molecular speciation of two sets of $NiO–MoO_3/Al_2O_3$ catalysts, containing 0–7% NiO with 7.5% MoO_3 or 15% MoO_3, is examined spectroscopically as a function of *in situ* O_2 calcination–H_2O exposure cycles. The sensitivity of ion scattering spectrometry to detect Mo in these catalysts is dependent upon their exposure to H_2O but is not dependent upon NiO concentration. This dependence, in conjunction with *in situ* Raman spectroscopic data, is used to describe sites of interaction of Ni or H_2O with the surface molybdate. These Ni–Mo and H_2O–Mo interactions are shown to be distinct and are discussed in relation to previously published data on the structure and HDS activity of $NiO–MoO_3/Al_2O_3$ catalysts.

Raman spectroscopic investigations of $NiO–MoO_3/Al_2O_3$ catalysts have provided fundamental insight into the molecular speciation that occurs as a function of metal oxide loadings, promoter concentrations, and the order of metals impregnation (*1–5*). Some investigations of $NiO–MoO_3/Al_2O_3$ have also included the use of multitechnique analyses that have provided invaluable correlations between the metal oxide dispersion, the chemical oxidation states, the metal oxide site symmetries, bulk compound formation, and subsequent behavior and speciation during H_2 reduction and H_2S sulfidation (*1–8*). Recent Raman spectroscopic studies of the molecular speciation in Al_2O_3-supported MoO_3, WO_3, and ReO_4 (*9–12*) have shown that highly dispersed molybdenum, tungsten, and rhenium oxides readily interact with H_2O and O_2 and that this interaction causes large shifts in the metal–oxygen stretching frequencies associated with these surface oxides. Such a dramatic effect has provided an explanation for the discrepancies between the spectral characteristics of supposedly identical MoO_3/Al_2O_3 and WO_3/Al_2O_3 catalysts (*9, 10*). In addition, these recent Raman results have led to a reevaluation of spectral interpretations that were based on an assumed dependency of the metal–oxygen stretching frequency upon symmetry or aggregate size of the surface metal oxide (*5, 12–15*); specifically, changes in the terminal Mo=O or W=O stretching frequencies in MoO_3/Al_2O_3 or WO_3/Al_2O_3 catalysts were found to be dependent upon the interaction of the surface metal oxide with adsorbates (*9–11*).

Spectroscopic data have indicated that in $NiO–MoO_3/Al_2O_3$, the Ni is incorporated into the two-dimensional surface molybdate species (*1–4, 14, 15*). Depending on sample preparation and subsequent calcination temperatures, $NiMoO_4$, $Al_2(MoO_4)_3$, or crystalline MoO_3 can also be formed (*2–4*). However, highly active $NiO–MoO_3/Al_2O_3$ catalysts do not normally contain these crystalline phases; instead, studies have suggested that the active sites for hydrodesulfurization of thiophene are NiMoS sites at the edges of two-dimensional molybdenum islands (*16–18*). In the present spectroscopic investigation, the molecular speciation of two sets of $NiO–MoO_3/Al_2O_3$ catalysts is examined as a function of *in situ* O_2 calcination and H_2O exposure. The in-

[1] Reference in this report to any specific product, process, or service is to facilitate understanding and does not necessarily imply its endorsement or favoring by the U.S. Department of Energy.

0021-9517/85 $3.00

corporation of Ni into the MoO_3/Al_2O_3 samples is shown to perturb the spectral characteristics of the Raman active Mo=O stretching vibrations. Such perturbations are discussed in relation to the structural characteristics of these catalysts and in relation to previous interpretations of data obtained on reduced and sulfided samples (*17, 18*).

EXPERIMENTAL

Sample preparation. The NiO–MoO_3/Al_2O_3 catalysts were prepared using Harshaw Al-4104E $\frac{1}{32}$-in., γ-Al_2O_3 extrudates (Harshaw Chemical Co.) having a surface area of approximately 200 m^2/g. The Al_2O_3 extrudates were ground with a mortar and pestle, and then sieved to −100 mesh. Water suspension and decantation were used to remove fines from the ground Al_2O_3. The Al_2O_3 was then dried overnight at 120°C. For Mo impregnation, a predetermined amount of $(NH_4)_6Mo_7O_{24} \cdot 4H_2O$ (Baker, Analyzed Reagent) was dissolved in distilled water, and this solution was used to saturate the dried Al_2O_3 to incipient wetness. The impregnated samples were allowed to sit at 25°C for $\frac{1}{2}$ h before subsequent calcination at 500°C for $\frac{1}{2}$ h. The samples were then impregnated with nickel nitrate, dried at 120°C, and calcined in air at 500°C for 16 h. These samples contained nominal concentrations of 15 wt% MoO_3 0–7 wt% NiO, and 7.5 wt% MoO_3 with 0–4 wt% NiO. Designations for the catalysts will be (0–7%)NiO–15%MoO_3/Al_2O_3 and (0–4%)NiO–7.4%MoO_3/Al_2O_3. Data in the figures will be plotted using concentrations of Ni and Mo determined by atomic absorption.

Spectral acquisition. The air-calcined, powdered catalysts were pressed into 13-mm-diameter wafers. These wafered samples were attached to a rotary feedthrough in a sample cell containing a quartz optical flat. This cell could be evacuated, flushed with selected gases, heated in a tubular furnace, and positioned at the entrance optics of the Raman spectrometer. Evacuation was facilitated with ultrahigh-vacuum, stainless-steel hardware having a turbomolecular pump as the primary pumping station. No vacuum grease was present in this system.

The cell permitted the environment of the catalysts to be controlled before and during spectral acquisition. Typically, a Raman spectrum of an air-exposed catalyst was obtained while the catalyst was in the cell. The cell containing the sample was then evacuated to $\sim 10^{-6}$ mbar, backfilled with 1000 mbar of O_2 (Matheson, Research Grade), and then heated at 500°C for 1 to 2 h. During this O_2 calcination, the sample cell was evacuated and backfilled with O_2 at least three times to ensure complete calcination. For catalysts exposed to distilled, deionized H_2O, the cell was evacuated to 10^{-6} mbar and then backfilled to 10–25 mbar of H_2O vapor while the sample was at 25°C.

The Raman spectra were recorded with the use of a Spex Ramalog spectrometer equipped with holographic gratings. A Spectra Physics Model 165 argon-ion laser was used to supply 45 mW at 514.5 nm to the rotating sample. The spectral slit width was maintained at 4 cm^{-1} throughout the experiments. Data handling was facilitated by use of a Spex Datamate.

Ion scattering spectrometry (ISS) data were obtained with a 3M Model 525 ISS/SIMS spectrometer by averaging 128 individual scans over a 5-min period. Isotopically pure ^4He (Monsanto Research Corp.) was used as the primary beam gas. The base pressure of the ISS/SIMS instrument was 1.3×10^{-9} mbar; spectra were acquired at a ^4He pressure of 5×10^{-5} mbar with 2 keV primary beam energy. The NiO–MoO_3/Al_2O_3 were pressed into thin 12-mm-diameter wafers; mounted on a retractable, sealable probe; and placed in the ISS vacuum chamber for analysis of the as-prepared samples. After data collection, the samples were removed from the ISS vacuum chamber and placed in a tube furnace for 500°C, O_2 calcination for 2 h. After cal-

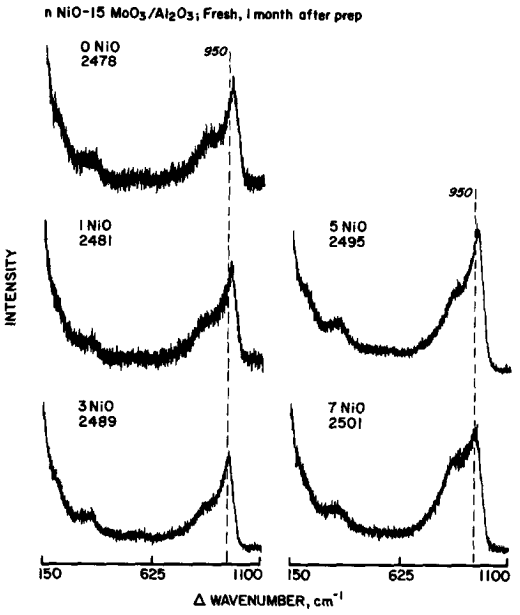

FIG. 1. Raman spectra of air-exposed (0–7%)NiO–15%MoO_3/Al_2O_3 1 month after catalyst synthesis.

cination, the probe was sealed for transport and insertion of the samples into the ISS analysis position. With conclusion of this O_2-calcined sample analysis, the catalysts were removed from the ISS chamber and exposed to 15 mbar of H_2O pressure for periods ranging from 2 h to 2 days. Again, the same samples were analyzed by ISS for comparison of elemental surface concentrations of these O_2-calcined, H_2O-exposed samples with the data from their previous as-prepared or O_2-calcined states. Different sample wafers were analyzed up to five times to ensure repeatability in elemental ratios. In addition, a different spot, approximately 1 mm in diameter, was selected on the catalyst wafers for successive analyses of the as-prepared, O_2-calcined, and H_2O-exposed samples.

RESULTS

Raman spectra of (0–7%)NiO–15% MoO_3/Al_2O_3 catalysts, obtained while the catalysts were exposed to atmospheric conditions and within 1 month of sample preparation, are shown in Fig. 1. The spectra of (0–4%)NiO–7.5%MoO_3/Al_2O_3 were qualitatively similar to those in Fig. 1. These types of spectra have been shown previously (*1*, *2*) and are presented to facilitate an ease of comparison with spectra of the same catalysts after *in situ* O_2 calcination, as shown in Fig. 2. Differences between the spectral characteristics in Figs. 1 and 2 include a decrease in relative intensity of bands at 210 and 350 cm^{-1} after O_2 calcination, and a shifting of the band at ca. 950 cm^{-1} (Fig. 1) to 1007 cm^{-1} after O_2 calcination (Fig. 2). An increase in the NiO concentration does not change significantly the positions or relative intensities of bands at 210 and 350 cm^{-1} for either the air-exposed or O_2-calcined catalysts.

To investigate spectral changes that occur with long-term atmospheric exposure of the catalysts, Raman spectra were obtained after the (0–7%)NiO–15%MoO_3/Al_2O_3 samples had been exposed to atmospheric conditions for 1 month and for 1 year. The regions 700–1100 cm^{-1} of these spectra are shown in Figs. 3 and 4, respectively. After 1 month of air exposure, the frequency of

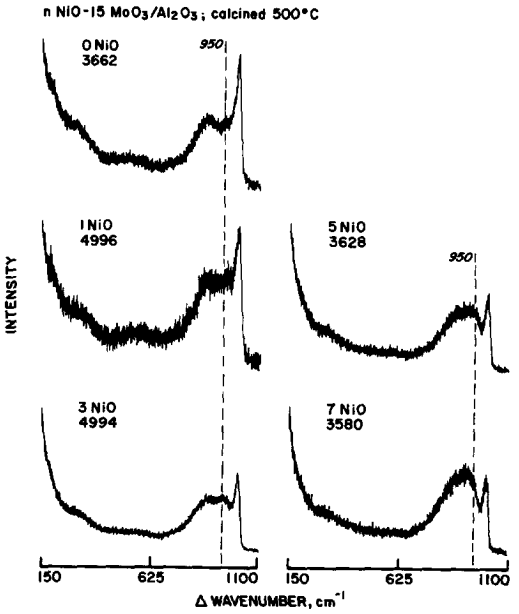

FIG. 2. Raman spectra of 500°C, O_2-calcined (0–7%)NiO–15%MoO_3/Al_2O_3.

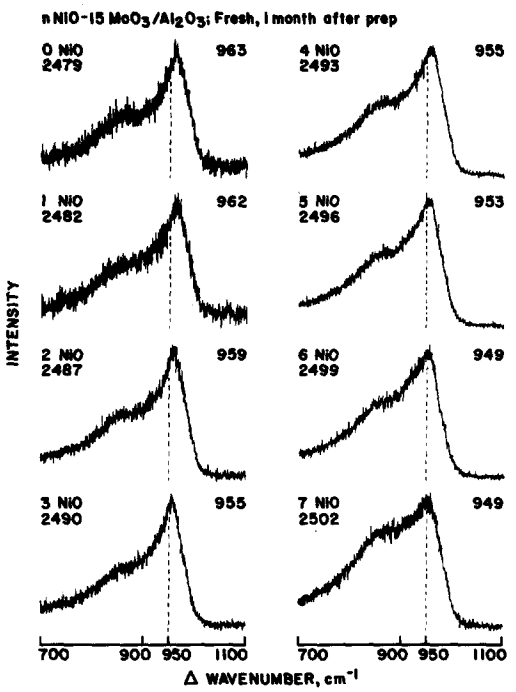

FIG. 3. Raman spectra of air-exposed (0–7%)NiO–15%MoO_3/Al_2O_3 1 month after catalyst synthesis.

the most intense peak varies from 963 to 949 cm^{-1}. The position of this band after 1 year of air exposure to the samples is approximately constant at 951 cm^{-1}, independent of NiO concentration. In addition to the differences in position of the most intense peak, the intensity and shape of the shoulder near 900 cm^{-1} are significantly different in Figs. 3 and 4.

The Raman spectra of the region 700 to 1100 cm^{-1} of 500°C, O_2-calcined (0–7%)NiO–15%MoO_3/Al_2O_3 samples are shown in Fig. 5. As shown in Fig. 6, the ratio of the integrated area (intensity) of the band at 1007 cm^{-1} to the integrated area (intensity) of the shoulder in the region 850 to 950 cm^{-1} [I(1000)/I(900)] decreases with increasing NiO concentration. However, the position of the 1007-cm^{-1} band is independent of the NiO concentration (Fig. 5). Distinct from this independence of band position upon NiO concentration is the continual shifting of the 1007-cm^{-1} band to lower frequencies with small, incremental dosing of H_2O. Exposure of the O_2-calcined catalysts to 15 Torr H_2O for 20 min causes the disappearance of the 1007-cm^{-1} band and the reappearance of an intense peak at 950 cm^{-1}. The spectra of these H_2O-exposed samples consist of band positions and intensities similar to those for the 1 year, air-exposed samples in Fig. 4. Repeated O_2-calcined, H_2O-exposure experi-

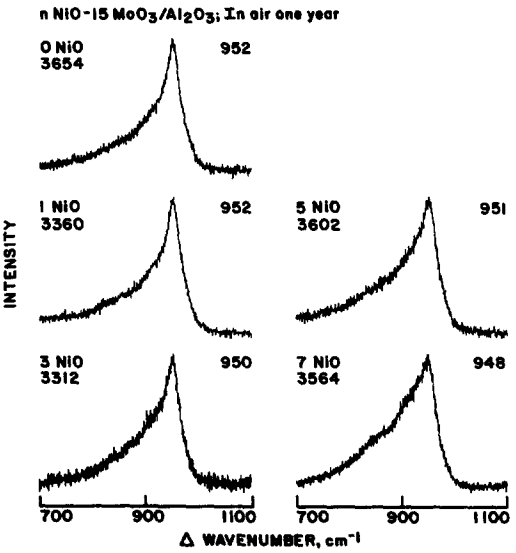

FIG. 4. Raman spectra of air-exposed (0–7%)NiO–15%MoO_3/Al_2O_3 1 year after catalyst synthesis.

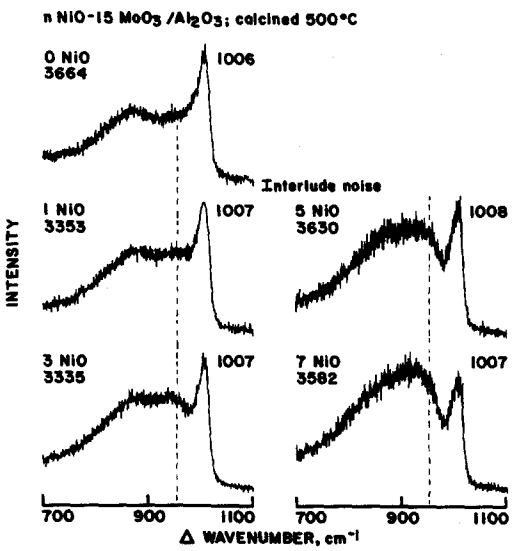

FIG. 5. Raman spectra of 500°C O_2-calcined (0–7%)NiO–15%MoO_3/Al_2O_3.

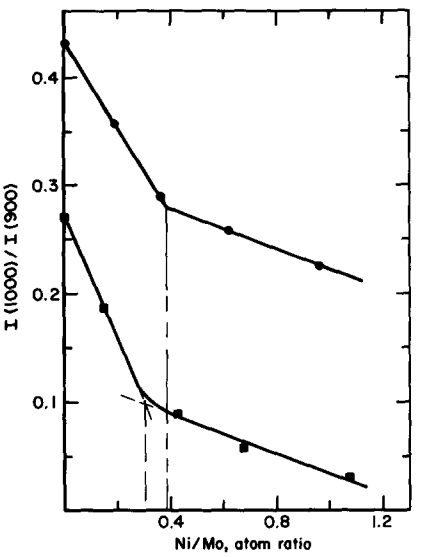

FIG. 6. The integrated intensity of the 1000-cm^{-1} band, $I(1000)$, ratioed to the integrated intensity of the band in the region 850 to 950 cm^{-1}, $I(900)$, as a function of NiO concentration for 500°C O_2-calcined catalysts. (●) (0–4%)NiO–7.5%MoO_3/Al_2O_3; (■) (0–7%)NiO–15%MoO_3/Al_2O_3.

ments on the same sample or on different samples with constant NiO concentrations show reversibility in band positions and intensities. In all cases, the exposure of O_2-calcined catalysts to H_2O restores the intensities of the 210- and 350-cm^{-1} bands to those shown in Fig. 1.

The same type of band reversibility, between 950 and 1004 cm^{-1}, during O_2-calcination and H_2O-exposure experiments was found for the (0–4%)NiO–7.5%MoO_3/Al_2O_3 samples. In addition, the intensity ratio $I(1000)/I(900)$ decreases with increasing NiO concentration, as shown in Fig. 6. The Ni/Mo atomic ratio at which the slopes in Fig. 6 change occurs at approximately 0.3 for the (0–7%)NiO–15%MoO_3 samples and at approximately 0.4 for the (0–4%)NiO–7.5%MoO_3 samples.

Figure 7 shows ISS data of Mo/Al intensity ratios as a function of NiO concentrations that were obtained during 5 min of ^4He bombardment. An estimate of the sputter rate is 0.05 nm/min, determined from ISS experiments of Mo coatings on Co substrates. These data show that the Mo/Al ratio is nearly independent of the NiO concentration. However, the Mo/Al intensity ratios are sensitive to the treatment received by the catalysts before data acquisition. In particular, the data for O_2-calcined samples have Mo/Al ratios nearly 50% larger than the data for as-prepared or H_2O-exposed samples. These ratios are dependent on the total time of ^4He sputtering before and during data collection. For example, the Mo/Al ratio decreases rapidly with sputter time, decreasing by as much as 40% in 10 min of sputter. The Ni/Al ratio increases linearly with increasing NiO concentration; this linearity is independent of the ^4He sputter time, whereas the absolute values of Ni/Al at a constant NiO concentration generally decrease with longer sputter periods.

DISCUSSION

The Raman spectral results in Figs. 1 through 5 show, as previously discussed (*9–11*), that shifts in frequency of the Mo=O stretching vibration cannot be interpreted unambiguously to be the result of different degrees of aggregation or symmetry of the surface molybdate when spectra are obtained with samples exposed to the atmosphere. Instead, the interaction of

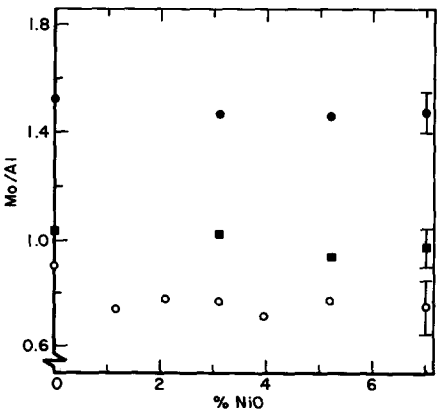

FIG. 7. The Mo/Al intensity ratios from ISS experiments on 1-year air-exposed catalysts (○), on 500°C O_2-calcined samples (●), and on O_2-calcined samples after H_2O exposure (■). (0–7%)NiO–15%MoO_3/Al_2O_3.

H_2O with the surface molybdate controls the frequency of the Mo=O stretching vibration when data are obtained on air-exposed catalysts; and as indicated from inspection of Figs. 1 and 2, H_2O controls the relative intensity of the bands in the region 200 to 350 cm^{-1}. Possibly, the interaction of H_2O with the surface molybdate induces a weakening of the molybdenum–oxygen force constants or changes the coordination number of the molybdenum.

The increased Mo/Al intensity ratios after O_2 calcination in Fig. 7 are related to an increase in the observability of the Mo and/or a decrease in the observability of the Al. Such changes in observability could be caused by a redispersion of the Mo over the Al_2O_3 during O_2 calcination. However, this type of mechanism should not produce decreased Mo/Al intensities after H_2O exposure at 25°C, nor is it expected to produce a 60-cm^{-1} shift in the Raman Mo=O vibrational frequency. Additionally, the Mo in these samples is highly dispersed upon catalyst preparation, as is evidenced by the absence of Raman and XRD spectral characteristics of crystalline MoO_3, $NiMoO_4$, $Al_2(MoO_4)_3$, or $NiAl_2O_4$. The relative sensitivity of Raman spectroscopy to observe crystalline MoO_3, Al_2MoO_4, and the surface molybdate species is approximately 100 : 5 : 1 (*19*). Hence, these data indicate that the changes in Mo/Al ISS data during O_2 calcination and H_2O exposure are not related to Mo or Al observability as a result of redispersion of the Mo.

Physical shielding of surface atoms by adsorbed species is a well-known phenomenon in surface-sensitive experimentation (*20*). Such obscuration of Mo will occur in the case of a H-bonded H_2O on the surface molybdate but will not occur in the case of hydrolysis of Mo–O–Al bonds. Instead, hydrolysis of Mo–O–Al bonds may cause physical shielding of Al by the formation of Al–OH species and thereby cause Mo/Al intensity changes opposite to the change observed, i.e., an increased Mo/Al intensity ratio after H_2O exposure and a decreased Mo/Al intensity ratio after O_2 calcination. Similarly, a tetrahedral-to-octahedral transformation as a result of H_2O exposure may increase the observability of Mo by ISS techniques (*20*). However, the presence of H_2O complicates such an interpretation. In the case of ReO_4/Al_2O_3, a system described as containing only tetrahedral ReO_4 species (*12*), the effect of H_2O on the position of the Raman Re=O vibrational modes is the same as H_2O on the Mo=O vibrational modes. Thus, in the present investigation, the interaction of H_2O by H-bonding/proton donation with the terminal oxygen of the surface molybdate could produce the spectral effects observed in the Raman and ISS data, whereas the effect of coordination expansion cannot be defined unambiguously, and the effect of hydrolysis of Mo–O–Al bonds would produce changes opposite those that are observed.

The trend of a more intense vibrational mode near 950 cm^{-1} and a correspondingly less intense mode near 1000 cm^{-1} with either H_2O addition to the calcined catalysts or Ni incorporation may imply that the net effect of H_2O on the Mo=O stretching vibration is similar to that of Ni. However, the shift in the Mo=O stretching vibrational frequency with H_2O addition is continuous, i.e., any band position between ca. 1000 cm^{-1} and ca. 950 cm^{-1} can be obtained by fractional doses of H_2O. The change caused by Ni incorporation is abrupt, i.e., band intensity at 1000 or near 950 cm^{-1} is affected by Ni. Hence, the effect of Ni on the Raman spectroscopic characteristics of the Mo=O stretching vibrations is dramatically different from the effect of H_2O. This difference implies that the interaction mechanism and/or the site of interaction of Ni with the Mo=O units is distinct from that of H_2O with the Mo=O units. For example, the effect of H_2O on the Mo=O vibrations could be the result of long-range interactions, as previously discussed for WO_3/Al_2O_3 (*10*), while the effect of Ni on the Mo=O vibrations could be the result of short-range interactions.

The capability to distinguish between such long-range and short-range interactions is dependent on the ability of Raman scattering to detect molecular vibrations having active modes within unique structural entities. In distinction from the Raman effect, detection of Mo by ISS provides information on the "average" observability of Mo over the entire surface. Still, the ISS data in Fig. 7 show that the addition of H_2O to the catalysts affects differently the Mo observability compared to the addition of Ni. According to the geometric model proposed by Kasztelan *et al.* (*16*) and the results of Bachelier *et al.* (*17, 18*), the molybdenum in sulfided Mo/Al_2O_3 is contained in small islands. The size of these islands is dependent on the Mo loading with approximately 17 atoms/island with a 7.5% MoO_3 loading. Such a model of the surface molybdate may have application in explaining the Raman and ISS data in the present investigation. For example, such islands contain crosslinked Mo–O–Mo structure when molybdena concentrations are above 5 wt% (*20, 21*). In addition, the interaction of the Mo with the surface of the Al_2O_3 produces heterogeneous Mo–O–Al bonding energies; as a consequence of this heterogeneity, the Mo–O stretching vibrations in the Mo–O–Al units could cover a broad range. The Mo–O stretching frequency in Mo–O–Mo bonds would be expected to occur in the same frequency region (700 to 900 cm^{-1}) as Mo–O stretching frequencies for Mo–O–Al bonds. As a result, a very broad band, as is observed in the region 800 to 900 cm^{-1} in Figs. 1 to 5, would be expected. Addition of H_2O and its subsequent interaction with oxygen in the surface molybdate of the calcined samples may not appreciably affect the force constants of these Mo–O–Mo or Mo–O–Al vibrational modes. In this case, the broad band in the region 800 to 900 cm^{-1} would not shift during O_2 calcination–H_2O exposure cycles; such independency is experimentally observed. This suggests that the Mo–O–Mo or Mo–O–Al bonds act as passive conduits for the long-range rearrangement of charge density within the terminal Mo=O bonds during O_2 calcination–H_2O exposure cycles. At low concentrations of Mo, these terminal Mo=O bonds would be associated with monomer and dimer molybdena species (*21*). As the Mo loading increases, and consequently as the size of the molybdena islands increases (*16*), the terminal Mo=O bonds may be associated with the edge of the molybdena islands. Such edge sites, consisting of unsaturated Mo (*16*), are more reactive than those Mo within the basal plane of the molybdena island.

The plots of the Raman intensity ratio [$I(1000)/I(900)$] versus Ni/Mo atomic ratio in Fig. 6 contain slope changes at Ni/Mo $\simeq$ 0.3 for (0–7%)NiO–15%MoO_3/Al_2O_3 and at Ni/Mo $\simeq$ 0.4 for (0–4%)NiO–7.5MoO_3/Al_2O_3. In the region Ni/Mo $>$ 0.4, the slopes of the lines are less than one fourth of the slopes of the lines when Ni/Mo $\leq$ 0.4. This change in slope suggests that when Ni/Mo $\geq$ 0.4, the amount of Ni interacting directly with the terminal Mo=O bonds is less per added amount of Ni than when Ni/Mo $\leq$ 0.4. The ability to obtain significant information from these plots concerning the incorporation of Ni is a consequence of minimal perturbation to the Mo–O–Mo and/or Mo–O–Al vibrations by Ni or by H_2O. Hence, the data in Fig. 6 compare intensities of highly interacting Mo=O bonds with stable Mo–O–Mo bridging bonds or with stable Mo–O–Al support-anchoring bonds. In relation to such an interpretation, the (0–4%)NiO–7.5%MoO_3/Al_2O_3 samples would be expected to contain fewer bridging and support-anchoring oxygen bonds relative to terminal oxygen in a molybdena island (*16, 20, 21*). In addition, the molybdena would cover less of the support in samples of lower concentrations of MoO_3. Therefore, the intensity ratio, $I(1000)/I(900)$, for (0–4%)NiO–7.5%MoO_3/Al_2O_3 should be larger than the intensity ratio for (0–7%)NiO–15%MoO_3/Al_2O_3. The values of Ni/Mo at which the slopes of the intensity plots

change for these two catalyst series are in close agreement with those values at which a maximum promotional effect of Ni is found for thiophene desulfurization using Ni–Mo/Al_2O_3 (*17, 18*).

Although the catalysts investigated herein are not in their sulfided state, the surface structure in the oxide form of these catalysts is expected to control the surface speciation in their sulfided state (*22, 23*). If so, the Ni that interacts directly with the terminal Mo=O bonds of the surface molybdate may be located at the edge of molybdena islands for these catalysts that contain a MoO_3 concentration greater than 7 wt%. If these catalysts were sulfided, the location of the catalytically active species may be NiMoS at the edge of MoS_2 islands (*17, 18*), similar to catalyst speciation in Mo/Al_2O_3 and Co–Mo/Al_2O_3 (*24–26*).

CONCLUSIONS

It has been shown that Raman vibrational spectroscopy can be used to detect Ni–Mo interactions when proper precautions are taken to ensure discernment between the effects of adsorbates, such as H_2O, and the effects of Ni incorporation. The ISS and Raman data on NiO–MoO_3/Al_2O_3 point to a direct interaction of Ni with Mo=O units at the edge of molybdena islands. Such a location would be favorable for the formation of edge Ni–Mo–S sites that form during catalyst sulfidation and that possess high catalytic activity. In addition, the effects of H_2O interacting with NiO–MoO_3/Al_2O_3 are the same as the effects of H_2O interacting with MoO_3/Al_2O_3 and WO_3/Al_2O_3.

ACKNOWLEDGMENTS

This work was funded in part by the Office of Basic Energy Science, under the Office of Energy Research, the Department of Energy. The authors also thank F. R. Brown, K. H. Rhee, and D. H. Finseth for stimulating discussions, and J. F. Paterline for the acquisition of the Raman data.

REFERENCES

1. Knözinger, H., Jeziorowski, H., and Taglauer, E., *in* "Proceedings, 7th International Congress on Catalysis, Tokyo, 1980," paper A42. Elsevier, Amsterdam, 1981.
2. Dufresne, P., Payen, E., Grimblot, J., and Bonnelle, J. P., *J. Phys. Chem.* **85,** 2344 (1981).
3. Payen, E., Dhamelincourt, M. C., Dhamelincourt, P., Grimblot, J., and Bonnelle, J. P., *Appl. Spectrosc.* **36,** 30 (1982).
4. Lopez Agudo, A., Gil, F. J., Calleja, J. M., and Fernandez, V., *J. Raman Spectrosc.* **11,** 454 (1981).
5. Kantschewa, M., Delannay, F., Jeziorowski, H., Delgado, E., Eder, S., Ertl, G., and Knözinger, H., *J. Catal.* **87,** 482 (1984).
6. Gil Llambias, F. J., Mendioroz, S., Ania, F., and Lopez Agudo, A., *Appl. Catal.* **8,** 335 (1983).
7. Garcia Fierro, J. L., Soria, J., and Lopez Agudo, A., *Appl. Catal.* **3,** 117 (1982).
8. Chiplunker, P., Martinez, N. P., Mitchell, P. C. H., *Bull. Soc. Chim. Belg.* **90,** 1319 (1981).
9. Stencel, J. M., Makovsky, L. E., Diehl, J. R., and Sarkus, T. A., *J. Raman Spectrosc.* **15,** 282 (1984).
10. Stencel, J. M., Makovsky, L. E., Sarkus, T. A., deVries, J., Thomas, R., and Moulijn, J. A., *J. Catal.* **90,** 314 (1984).
11. Chan, S. S., Wachs, I. E., Murrell, L. L., Wang, L., and Hall, W. K., *J. Phys. Chem.* **88,** 583 (1984).
12. Wang, L., and Hall, W. K., *J. Catal.* **82,** 117 (1983).
13. Wang, L., and Hall, W. K., *J. Catal.* **66,** 251 (1980).
14. Sombret, B., Dhamelincourt, P., Wallart, E., Muller, A. C., Bouquet, M., and Grosmangin, J., *J. Raman Spectrosc.* **9,** 291 (1980).
15. Thomas, R., Mittelmeyer-Hazeleger, M. C., Kerhof, F. P. J. M., Moulijn, J. A., Medema, J., and de Beer, V. H. J., *in* "Proceedings, 3rd International Conference on Chemistry Uses of Molybdenum" (H. F. Barry and P. C. Mitchell, Eds.), pp. 85–91. 1979.
16. Kasztelan, S., Toulhoat, H., Grimblot, J., and Bonnelle, J. P., *Appl. Catal.* **13,** 127 (1984).
17. Bachelier, J., Duchet, J. C., and Cornet, D., *J. Catal.* **87,** 283 (1984).
18. Bachelier, J., Tilliett, M. J., Duchet, J. C., and Cornet, D., *J. Catal.* **87,** 292 (1984).
19. Baltrus, J., Makovsky, L. E., Stencel, J. M., and Hercules, D. M., submitted for publication.
20. Zingg, D. S., Makovsky, L. E., Tischer, R. E., Brown, F. R., and Hercules, D. M., *J. Phys. Chem.* **84,** 2898 (1980).

21. Li, C. P., and Hercules, D. M., *J. Phys. Chem.* **88,** 456 (1984).
22. Massoth, F. E., "Advances in Catalysis," Vol. 27, p. 265. Academic Press, New York, 1978.
23. Makovsky, L. E., Stencel, J. M., Brown, F. R., Tischer, R. E., and Pollack, S. S., *J. Catal.* **89,** 334 (1984).
24. Topsøe, H., Clausen, B. S., Candia, R., Wivel, C., and Mørup, S., *J. Catal.* **68,** 433 (1981).
25. Wivel, C., Candia, R., Clausen, B. S., Mørup, S., and Topsøe, H., *J. Catal.* **68,** 453 (1981).
26. Topsøe, H., Clausen, B. S., Cania, R., Wivel, C., and Mørup, S., *Bull. Soc. Chim. Belg.* **90,** 1189 (1981).